

Borrelia burgdorferi Tolerance-Associated Changes in Gene Expression of Murine Macrophages

Sophia Chen¹, Ricki Deng¹, Anis Hadi¹, Sara Nandwana¹, William G. Ryan V², John B. Presloid², R. Mark Wooten³

¹Summer Biomedical Science Program in Bioinformatics, Department of Neurosciences, University of Toledo College of Medicine and Life Sciences, Toledo, OH USA

²Graduate Student, Department of Neurosciences, University of Toledo College of Medicine and Life Sciences, Toledo, OH USA

³Department of Medical Microbiology and Immunology, University of Toledo College of Medicine and Life Sciences, Toledo, OH USA

Email: William.Ryan2@rockets.utoledo.edu

Received: 2024-12-17

Accepted for publication: 2025-01-22

Published: 05 February 2025

Abstract

Lyme disease, caused by the spirochete *Borrelia burgdorferi* (*Bb*), is the most prevalent vector-borne disease in the United States. Macrophages, key cellular players in the innate immune response, exhibit diminished functionality over time during *Bb* infection, potentially leading to chronic infection. This study explores the transcriptional changes associated with macrophages that develop tolerance to *Bb*. Using RNA sequencing of murine bone marrow-derived macrophages exposed to *Bb*, we identified differentially expressed genes and dysregulated pathways between productively stimulated and tolerized macrophages. Key findings revealed significant downregulation of type-I interferon signaling and associated immune responses, suggesting mechanisms of immune tolerance. Additionally, connectivity analysis identified potential drug candidates for repurposing to enhance macrophage activity. Our results underscore the complexity of macrophage responses to *Bb* and provide a foundation for future research to develop targeted therapies aimed at modulating immune responses and improving treatment outcomes for Lyme disease patients. Ultimately, these findings offer new insights into the pathogenesis and potential treatment strategies for Lyme disease.

Keywords: *Borrelia burgdorferi*, Lyme disease, macrophage, tolerance, transcriptional profiling, drug discovery

1. Introduction

1.1. Overview of Lyme Disease

First documented in Lyme, Connecticut, Lyme disease is an infectious disease caused by the spirochetal bacteria *Borrelia burgdorferi* (*Bb*).

The bacterium is spread to humans through the bite of Ixodes ticks, most commonly found in the northeastern and north central regions of the United States (2). A notable symptom to identify Lyme disease is an erythema migrans skin rash in the shape of a bullseye that emanates from the tick bite site and is sufficient for diagnosis of

a *Bb* infection in endemic areas. Other notable but less obvious acute symptoms include fatigue, headache, and fever (2). Even after antibiotic treatments that eventually clear the bacteria, symptoms of the disease can persist. These patients may continue to feel extreme fatigue, muscle pain, and have trouble thinking and performing daily tasks.

1.2. Health Impacts of Lyme Disease

Lyme disease has an estimated 500,000 cases per year in the United States, making it by far the most common vector-borne disease (3). Two different presentations of Lyme disease are diagnosed: acute and chronic. Acute disease has milder symptoms, with symptoms usually disappearing within a week, even without antibiotic treatment. Patients with acute Lyme disease usually make a full recovery if the infection is caught and treated with antibiotic intervention early. However, nearly 20% of patients may go on to develop chronic Lyme disease months later if not appropriately treated. These patients often develop more severe symptoms, including fatigue, muscle aches, arthritis, neurologic deficits, cardiac dysfunction, and increased sensitivity to light and sound (4). Chronic symptoms can continue to persist for many years even after antibiotic treatment, as patients may not experience complete recovery for years. These symptoms have a debilitating impact on a person's daily life. In a case study examining the neurological impacts of chronic Lyme disease symptoms on 24 patients with Lyme disease, 14 of them had memory impairment on neuropsychological tests (5). In 2018, the estimated cost of treating acute Lyme disease in the United States was \$4.8 billion, while chronic Lyme disease treatment cost an additional \$9.6 billion (6). Patients also reported an estimated cost of \$2,000 on average to treat Lyme disease per person (7), showing the financial burden that Lyme disease treatment places on individuals, their families, and the health care system.

1.3. Immune Response to Lyme Disease

After a tick bite, *Bb* enters the dermal tissues of the host. Here, the "first line of defense" of the body is enacted: the innate immune system. The

first innate immune cells *Bb* will likely encounter in the dermis are skin-resident macrophages. Macrophages are specialized white blood cells which recognize and scavenge foreign materials, including bacteria such as *Bb* (8). When a macrophage identifies signals that bacteria are present in the system, it will typically migrate to and engulf the bacterium to begin to break it down and kill it. In addition, it secretes soluble mediators that promote the influx of important immune cells from the bloodstream, which are usually needed to completely clear the infection (9).

1.4. Macrophage Tolerance to *Bb* Clearance

Macrophages use several different receptors and signaling pathways to detect bacteria, including Toll-like receptor 2 (TLR2), the FcγR-receptor and complement receptor-3 (9). When *Bb* enters a host, macrophages sense soluble and surface molecules from the bacterium and move towards it to engulf and kill the *Bb*. However, *Bb* moves at about 10 micrometers per second due to its spirochetal shape and powerful endoflagella, allowing it to move faster than most immune cells, including macrophages (10). In addition to this speed, *Bb* can rapidly sense the environment and change directions, making it incredibly difficult for macrophages and other immune cells to capture the bacteria (11). While macrophages initially appear to efficiently recruit other cells into the area to help clear the infection, over time this recruitment diminishes. A potential explanation for this is that the macrophages are becoming tolerant and no longer recognizing that they need to promote inflammatory responses to clear this infection (1). Thus, while *Bb* is still present in the host, macrophages are no longer acting efficiently to support immune clearance of the persisting bacteria. Therefore, there is great interest in identifying the mechanisms that cause macrophages to cease to efficiently promote immune clearance of *Bb*, so that proper function could be restored and decrease the development of persistent infection and chronic Lyme disease symptoms.

1.5. Transcriptional Assessment of Infection-Induced Mechanisms

Previously, immune tolerance of macrophages in vitro has been studied with enzyme-linked immunosorbent assays (ELISA) by Chung et al. (12). However, the main drawback of sandwich ELISAs is that they usually assess an individual protein target on a particular assay. This means that all other proteins which may be playing a role in infection-induced mechanisms are not assessed. Alternatively, using transcriptional profiling to assess the entire macrophage transcriptome allows for an unbiased analyses of gene regulation (13). The main purposes of this method include diagnosing diseases, planning/creating treatments for diseases, and evaluating how well a treatment is working in some cases (14). In hosts with Lyme disease, we hypothesized that extended exposure to *Bb* causes a subset of macrophage genes to be downregulated, decreasing macrophage functionality to eliminate *Bb*, and therefore creating a tolerance to the infection. Our goal was to elucidate the mechanism(s) within macrophages that suppresses their ability to clear the bacteria by testing macrophage response to single versus multiple stimulations of *Bb* using RNA sequencing (RNAseq). Here, we analyzed differential gene expression using previously collected RNAseq datasets in control and experimental groups of mouse-derived macrophages treated in vitro with and without *Bb* (1).

2. Methods

2.1. Macrophage Isolation and Treatment

This work was performed previously as described by Petnicki-Ocwieja et al. (1) (**Figure 1**). All experiments were approved by Tufts Institutional and Animal Care Committee. Macrophages were expanded from the bone marrow of wild-type mice (C57BL/6J), which are known as marrow-derived macrophages (BMDMs). Briefly, bone marrow was dissociated into 100 mm x 15 mm Petri dishes with sterile DMEM containing 30% L929 cell conditioned medium as the growth factor medium, 20% FBS, and 1% penicillin-streptomycin for 5-7 days, which generates BMDMs. Six plates with 2 x 10⁶ BMDMs each were separated into three groups (n=2): one control and two experimental groups

stimulated with *Bb* (B31 or N40 strains). The control group contained unstimulated BMDMs as a baseline comparison. The second group was co-cultured with *Bb* for 6 hours, which represents the initial response of macrophages to *Bb* stimulation during infection (i.e. "stimulated"). The third group was comprised of BMDMs stimulated for 24 hours with *Bb*, washed, then restimulated with *Bb* for 6 hours, representing the responses of macrophages which have had a previous encounter with *Bb* (i.e. "re-stimulated" or "tolerized").

2.2. Generation of RNAseq Library

Macrophage responses were observed by measuring gene expression with RNAseq after 0, 6, and 30 (24+6) hours post-treatment (GSE236149) as described above. After treating harvested cells with TRIzol, libraries were prepared using reagents by Genewiz Inc and sequenced with Illumina HiSeq 4000 at an estimated 25 million reads per sample. Using STAR, the RNAseq reads were aligned to the mm10 mouse reference genome, and RSEM was used to quantify the reads. Differential gene expression analyses were conducted in R using edgeR and voomLmFit. Genes having a FDR-adjusted p-value of < 0.05 were considered significant.

2.3. Bioinformatics Analyses

Our study used a publicly-available R programming language software package (3PodReports) to analyze the publicly collected gene expression data sets (1), which included the gene symbols, log2FoldChange, p-value, and adjusted p-value. 3PodR generates a HTML-format interactive web report, including the results of pathway analyses like Gene Set Enrichment Analysis (GSEA), and computational drug discovery analyses were performed using iLINCS (**Figure 1**) (15-17). Pathways having an FDR adjusted p-value of < 0.05 were considered significant and clustered into biological themes with PAVER (18).

3. Results

3.1. *Bb*-Mediated Activation vs Tolerance-Associated Gene Expression Signatures

A heatmap depicting the combined top 50 upregulated and downregulated genes by absolute log₂ fold change in both the stimulated (6 hr) vs. control (C) groups and the restimulated (24 hr) vs. stimulated (6 hr) groups are shown in **Figure 2A** and **Table S1**.

For the initial activation of macrophages by *Bb* (6hr vs. control groups), the heatmap indicated large numbers of upregulated genes and a smaller subset of downregulated genes. Notable genes in this upregulated group include IL-12 α and β , IL-6, CD69, IL-1 α , and many other proinflammatory cytokines that have been previously identified to be upregulated by macrophages when exposed to *Bb* in vitro (10). Alternatively, in the macrophages that were restimulated to elicit *Bb*-induced tolerance (24 hr vs. 6 hr groups), analysis shows a much larger subset of downregulated genes compared to upregulated genes. Many of these significantly downregulated genes are the same inflammatory genes that were significantly upregulated in the *Bb*-stimulated populations. Plotting log₂ fold change vs log p value allows construction of volcano plots to identify specific genes with significant differences in regulation. Among the stimulated groups vs unstimulated controls, families of inflammatory mediators are significantly upregulated, including interleukins, chemokines and chemokine receptors, and interferon-activated genes (**Figure 2B**).

Conversely, comparing restimulated to stimulated groups, notable genes such as *Sipi*, *Susd2*, and *Adh7* are significantly upregulated, while downregulated genes include *Ngp*, *Kif18b*, and *Gm42742* (**Figure 2C**).

3.2. Unsupervised Pathway Clustering Identifies Specific Interferon Dysregulation

Our Gene Set Enrichment Analysis (GSEA) was performed to get a more systems-level assessment of these changes under stimulatory vs tolerance-induced populations. For the 6hr vs control group, a total of 816 significantly altered pathways were identified. Of these 816 pathways, 699 were significantly upregulated while 117 were significantly downregulated. Some of the top upregulated pathways include defense response to other organisms, response

to bacteria, and regulation of response to pathogenic stimuli. Some of the top downregulated pathways include cilium, DNA repair, and cilium organization (**Figure 3, Table S2, Table 1**).

A total of 737 significantly altered pathways were identified between the 24hr vs 6hr groups. Of these 737 significant pathways, 173 were significantly up-regulated while 564 were significantly down-regulated. Some of the top upregulated pathways include oxoacid metabolic process, carboxylic acid metabolic process, and organic acid metabolic process. Some of the top down-regulated pathways include inflammatory responses to other organisms, viruses, and other pathogens (**Figure 3, Table S2, Table 1**).

3.3. Connectivity Analysis Identifies Candidate Repurposable Small Molecules

The Library of Integrated Network-based Signatures (LINCS) database was used to identify candidate repurposable drug therapies that potentially could reverse the effect of *Bb*-induced tolerance in macrophages. In our 24hr vs 6hr group, 2368 and 523 L1000 chemical perturbagen signatures in the LINCS database were identified as positively or negatively correlating to our gene signature, respectively (**Table S3**). The top 3 concordant (i.e. positively aligning) perturbagens were PHA-793887, Palbociclib, and Cladribine, while the top 3 discordant (i.e. negatively aligning) perturbagens were SCHEMBL1564574, VU0365118-1, and Parbendazole. We identified a total of 563 unique concordant mechanisms of action (MoA) and 201 unique discordant MoA in the 24hr vs 6hr group. The top MoA for 24hr vs 6hr concordant signatures includes VEGFR inhibitor, PDGFR tyrosine kinase receptor inhibitor and HDAC inhibitor (**Table 2**), while the top MoAs for discordant signatures include tubulin inhibitor, phosphodiesterase inhibitor, and adrenergic receptor agonist (**Table 3**).

In our 6hr vs. Control group, 2960 and 950 L1000 chemical perturbagen signatures in the LINCS database were identified as positively or negatively correlating to our gene signature, respectively (**Table S4**). The top 3 concordant

perturbagens were Nilotinib, Avicin-D, and Oxetane, while the top 3 discordant perturbagens were GSK-3 Inhibitor IX, ChEMBL2143694, and Loperamide. We identified 648 unique concordant MOAs and 273 discordant MOAs. The top 10 concordant MOAs included the dopamine receptor antagonist, VEGFR inhibitor, FLT3 inhibitor, HDAC inhibitor, serotonin receptor antagonist, PDGFR tyrosine kinase receptor inhibitor, CDK inhibitor, glutamine receptor antagonist, KIT inhibitor, and the adrenergic receptor antagonist. Top 10 discordant MOAs included glucocorticoid receptor agonist, acetylcholine receptor antagonist, PI3K inhibitor, adrenergic receptor antagonist, tubulin inhibitor, dopamine receptor agonist, KIT inhibitor, VEGFR inhibitor, PI3-kinase class 1 inhibitor, and PDGFR tyrosine kinase receptor inhibitor.

4. Discussion

4.1. Overview of Research

We investigated the transcriptional changes in macrophages induced by *Bb*, the spirochetal bacterium that caused Lyme disease in humans. Using RNA sequencing along with advanced bioinformatics approaches including STAR, Illumina and edgeR, our study identified differentially expressed genes in macrophages under single (i.e. initial activation; proinflammatory) vs repeated *Bb* stimulations (i.e. induction of tolerance) at optimal times for these conditions. To analyze our gene sequencing results, the R software package 3PodR was used, and key findings reveal that macrophages exhibit a complex transcriptional profile, including both upregulated and downregulated genes, suggesting mechanisms of immune tolerance and inflammation suppression. Using GSEA combined with PAVER, we identified several clusters of pathways with some previously implicated following repeated *Bb* stimulation, including type-1 interferon response and regulation of T cell proliferation, which suggest mechanisms of immune modulation and inflammation suppression in Lyme disease.

4.2. Interferon and Lyme Pathogenesis

Type-I interferon response signaling is one of the strongest correlates with severe cases of Lyme disease Lyme pathogenesis; both patients and/or mouse strains that exhibit severe Lyme-associated pathology display significantly increased production of type-I interferon. *Bb* induces the production of type-I interferon responses (19-21). In general, macrophages produce type-I interferons to defend against bacteria and viruses, particularly those that persist intracellularly. An activated macrophage can produce autocrine or paracrine signaling to neighboring cells to activate or suppress genes, leading to both positive and detrimental effects (22). However, *Bb* can elicit type-I interferon responses that can also lead to further Lyme disease-related complications (23). This is likely counterproductive to clearing these infections, as *Bb* persists extracellularly in dense tissues and mouse models that block type I IFN activation pathways exhibit less severe pathology compared to wild type mice (19). Previous research also shows type-I interferon responses inducing downstream cell signaling pathways when type-I interferons bind to their receptor (IFNAR), and therefore having a significant impact on a variety of biological effects (24).

4.3. Why Macrophages Become Tolerized to *Bb*

Using GSEA, we selected three genes of interest which were all significantly upregulated: *slpi*, *susd2*, and *adh* (13). *Slpi* is involved with the immune response, with its best described purpose being protecting epithelial surfaces from bacterial threat using endogenous proteolytic enzymes (25). *Susd2* is a gene which is involved in the negative regulation of cell division (26). *Adh* plays a role in metabolizing a bulk of the ethanol consumed in a diet (27). Using PAVER with GSEA, we identified a cluster of interest, the type-I interferon cluster. Within the type-I interferon cluster, 41 different pathways were identified using transcriptional profiling. Amongst these, the 3 with the greatest difference in pathway regulation include: positive regulation of cytokine production, positive regulation of interleukin-1 beta

production, and regulation of interleukin-1 beta production (**Table 1**). Type-I interferon is known to be a major contributor to the immune response, promoting antiviral effects in multiple non-immune and immune cell types, as well as in the development of CD4+ T cells (28, 29). As shown in Figure 3, the regulation of type-I interferon production is significantly decreased, indicating a correlation between type-I interferon and macrophage response to *Bb*. Since type-I interferon is being downregulated significantly, innate cells are lacking activation signals and T-cells are not developing as needed, which could explain the decrease in macrophage responses since certain T-cells types would likely lack activation in response to chronic *Bb* infection.

5. Conclusion

Our study provides significant insights into the transcriptional changes in macrophages induced by *Bb* and highlights the role of type-I interferon in modulating immune responses during Lyme disease, both during initial acute responses and in the more chronic development in tolerance. We identified key genes and pathways involved in macrophage tolerance, including the downregulation of interferon signaling. However, limitations such as the use of a single mouse strain and in vitro conditions may affect the generality of our findings. Future work should focus on validating these results in diverse models and investigating potential therapeutic interventions, such as those presented in **Table 3**, that target identified pathways to enhance macrophage function and reduce *Bb* persistence in Lyme disease.

References

- Petnicki-Ocwieja, T., J.E. McCarthy, U. Powale, P.K. Langston, J.D. Helble, and L.T. Hu, *Borrelia burgdorferi* initiates early transcriptional re-programming in macrophages that supports long-term suppression of inflammation. *PLOS Pathogens*, 2023. **19**(12): p. e1011886.
- Prevention, U.S.C.f.D.C.a. *About Lyme Disease*. 2024 [cited 2024 8/5/2024]; Available from: <https://www.cdc.gov/lyme/about/index.html>.
- Bohe, J.R., B.L. Jutras, E.J. Horn, M.E. Embers, A. Bailey, R.L. Moritz, Y. Zhang, M.J. Soloski, R.S. Ostfeld, R.T. Marconi, J. Aucott, A. Ma'ayan, F. Keesing, K. Lewis, C. Ben Mamoun, A.W. Rebman, M.E. McClune, E.B. Breitschwerdt, P.J. Reddy, ..., and B.A. Fallon, *Recent Progress in Lyme Disease and Remaining Challenges*. *Frontiers in Medicine*, 2021. **8**.
- Diseases, N.I.o.A.a.I. *Chronic Lyme Disease*. 2018 [cited 2018 8/5/2024].
- Logigian, E.L., R.F. Kaplan, and A.C. Steere, *Chronic neurologic manifestations of Lyme disease*. *N Engl J Med*, 1990. **323**(21): p. 1438-44.
- Davidsson, M., *The Financial Implications of a Well-Hidden and Ignored Chronic Lyme Disease Pandemic*. *Healthcare*, 2018. **6**(1): p. 16.
- Hook, S.A., S. Jeon, S.A. Niesobecki, A.P. Hansen, J.I. Meek, J.K.H. Bjork, F.M. Dorr, H.J. Rutz, K.A. Feldman, J.L. White, P.B. Backenson, M.B. Shankar, M.I. Meltzer, and A.F. Hinckley, *Economic Burden of Reported Lyme Disease in High-Incidence Areas, United States, 2014-2016*. *Emerg Infect Dis*, 2022. **28**(6): p. 1170-1179.
- Hirayama, D., T. Iida, and H. Nakase, *The Phagocytic Function of Macrophage-Enforcing Innate Immunity and Tissue Homeostasis*. *Int J Mol Sci*, 2017. **19**(1).
- Woitzik, P. and S. Linder, *Molecular Mechanisms of Borrelia burgdorferi Phagocytosis and Intracellular Processing by Human Macrophages*. *Biology (Basel)*, 2021. **10**(7).
- Bockenstedt, L.K., R.M. Wooten, and N. Baumgarth, *Immune Response to Borrelia: Lessons from Lyme Disease Spirochetes*. *Curr Issues Mol Biol*, 2021. **42**: p. 145-190.
- Shi, W., Z. Yang, Y. Geng, L.E. Wolinsky, and M.A. Lovett, *Chemotaxis in Borrelia burgdorferi*. *J Bacteriol*, 1998. **180**(2): p. 231-5.
- Chung, Y., N. Zhang, and R.M. Wooten, *Borrelia burgdorferi elicited-IL-10 suppresses the production of inflammatory mediators, phagocytosis, and expression of co-stimulatory*

receptors by murine macrophages and/or dendritic cells. PLoS One, 2013. **8**(12): p. e84980.

13. Illumina, I. *Reveal mechanisms of cell activity through gene expression analysis*. 2024 [cited 2024 8/5/2024].

14. Institute, N.C. *Gene expression profile*. 2011 [cited 2011.]

15. Korotkevich, G., V. Sukhov, N. Budin, B. Shpak, M.N. Artyomov, and A. Sergushichev, *Fast gene set enrichment analysis*. bioRxiv, 2021: p. 060012.

16. Pilarczyk, M., M. Fazel-Najafabadi, M. Kouril, B. Shamsaei, J. Vasiliauskas, W. Niu, N. Mahi, L. Zhang, N.A. Clark, Y. Ren, S. White, R. Karim, H. Xu, J. Biesiada, M.F. Bennett, S.E. Davidson, J.F. Reichard, K. Roberts, V. Stathias, A. Koleti, D. Vidovic, D.J.B. Clarke, S.C. Schürer, A. Ma'ayan, J. Meller, and M. Medvedovic, *Connecting omics signatures and revealing biological mechanisms with iLINCS*. Nature Communications, 2022. **13**(1): p. 4678.

17. Ryan, W., *willgryan/3PodR_bookdown: Pre-release for Zenodo DOI*. 2023, Zenodo.

18. Ryan V, W.G., A.S. Imami, H. Eby, J. Vergis, X. Zhan, J. Meller, R. Shukla, and R. McCullumsmith, *Interpreting and visualizing pathway analyses using embedding representations with PAVER*. Bioinformatics, 2024. **20**(7): p. 700-704.

19. Miller, J.C., Y. Ma, J. Bian, K.C. Sheehan, J.F. Zachary, J.H. Weis, R.D. Schreiber, and J.J. Weis, *A critical role for type I IFN in arthritis development following Borrelia burgdorferi infection of mice*. J Immunol, 2008. **181**(12): p. 8492-503.

20. Ma, Y., K.K. Bramwell, R.B. Lochhead, J.K. Paquette, J.F. Zachary, J.H. Weis, C. Teuscher, and J.J. Weis, *Borrelia burgdorferi arthritis-associated locus Bbaa1 regulates Lyme arthritis and K/BxN serum transfer arthritis through intrinsic control of type I IFN production*. J Immunol, 2014. **193**(12): p. 6050-60.

21. Paquette, J.K., Y. Ma, C. Fisher, J. Li, S.B. Lee, J.F. Zachary, Y.S. Kim, C. Teuscher, and J.J. Weis, *Genetic Control of Lyme Arthritis by Borrelia burgdorferi Arthritis-Associated Locus 1 Is Dependent on Localized Differential Production of IFN-beta and Requires Upregulation of Myostatin*. J Immunol, 2017. **199**(10): p. 3525-3534.

22. Adler, B. and H. Adler, *Type I interferon signaling and macrophages: a double-edged sword?* Cell Mol Immunol, 2022. **19**(9): p. 967-968.

23. Krupna-Gaylord, M.A., D. Liveris, A.C. Love, G.P. Wormser, I. Schwartz, and M.M. Petzke, *Induction of Type I and Type III Interferons by Borrelia burgdorferi Correlates with Pathogenesis and Requires Linear Plasmid 36*. PLOS ONE, 2014. **9**(6): p. e100174.

24. McNab, F., K. Mayer-Barber, A. Sher, A. Wack, and A. O'Garra, *Type I interferons in infectious disease*. Nature Reviews Immunology, 2015. **15**(2): p. 87-103.

25. Information, N.C.f.B. *SLPI secretory leukocyte peptidase inhibitor [Homo sapiens (human)]*. 2024 7/31/2024 [cited 2024].

26. Zhang, S., N. Zeng, N. Alowayed, Y. Singh, A. Cheng, F. Lang, and M.S. Salker, *Downregulation of endometrial mesenchymal marker SUSD2 causes cell senescence and cell death in endometrial carcinoma cells*. PLOS ONE, 2017. **12**(8): p. e0183681.

27. Edenberg, H.J., *The genetics of alcohol metabolism: role of alcohol dehydrogenase and aldehyde dehydrogenase variants*. Alcohol Res Health, 2007. **30**(1): p. 5-13.

28. Murira, A. and A. Lamarre, *Type-I Interferon Responses: From Friend to Foe in the Battle against Chronic Viral Infection*. Frontiers in Immunology, 2016. **7**.

29. Huber, J.P. and J.D. Farrar, *Regulation of effector and memory T-cell functions by type I interferon*. Immunology, 2011. **132**(4): p. 466-74

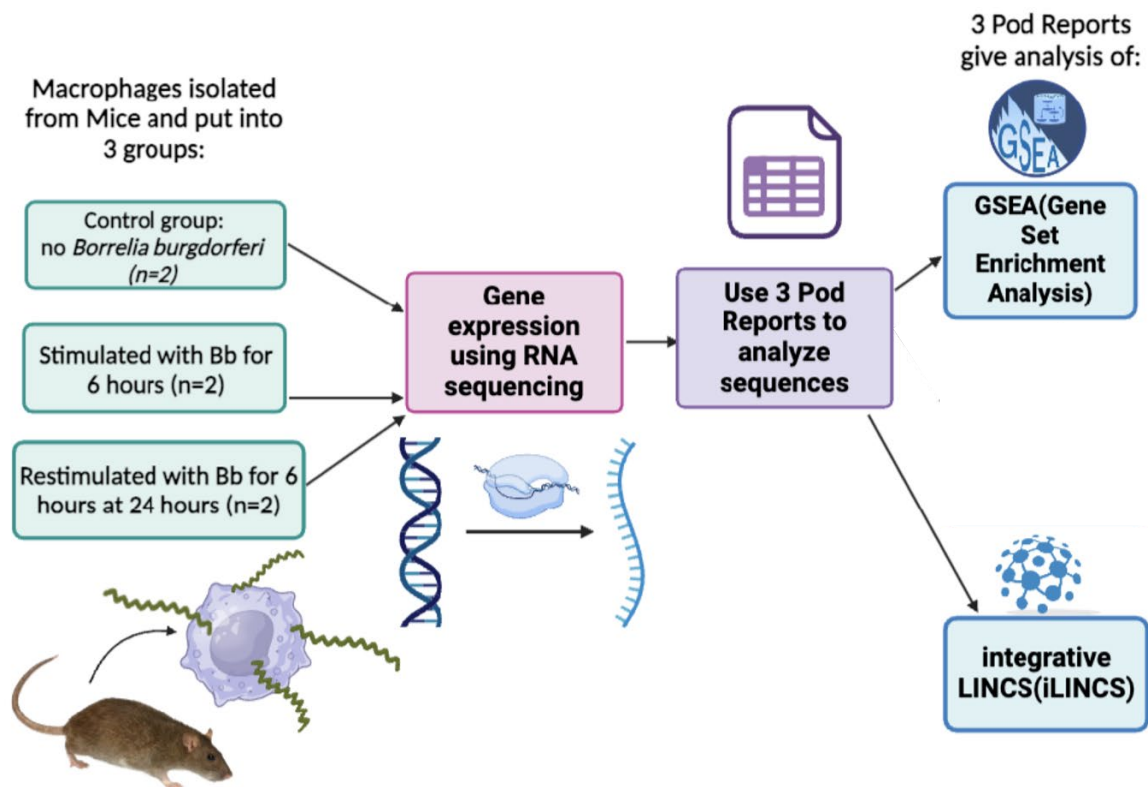


Figure 1. Workflow of the original study by Petnicki-Ocwieja et al. (1). BMDM were generated from mice and separated into three groups (n=2). The first group was a control group where no *Borrelia burgdorferi* (Bb) was administered. The second group was co-cultured with Bb for six hours. The third group was co-cultured with Bb for twenty-four hours, washed, and then restimulated for six hours before harvest. The gene expression of the macrophages was observed using RNA sequencing. Then, the differential expression results were analyzed using 3PodR and compared using GSEA and iLINCS. Created with BioRender.com.

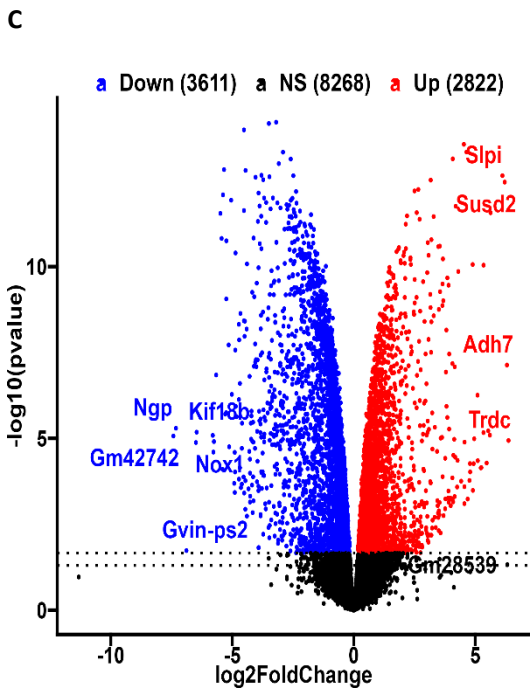
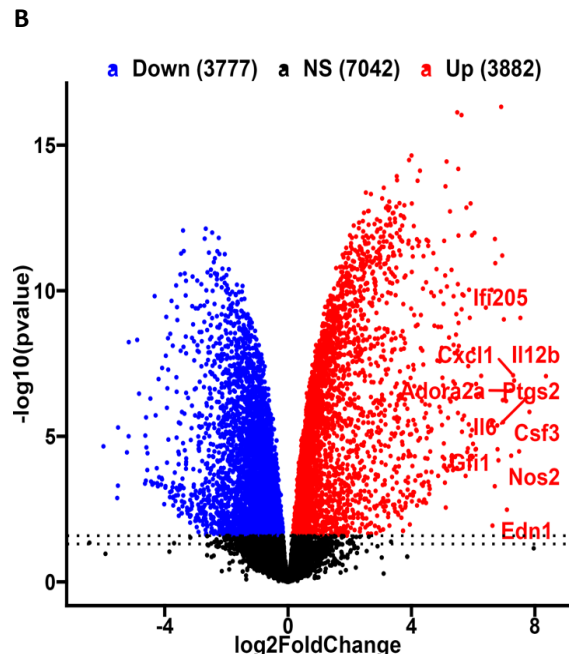
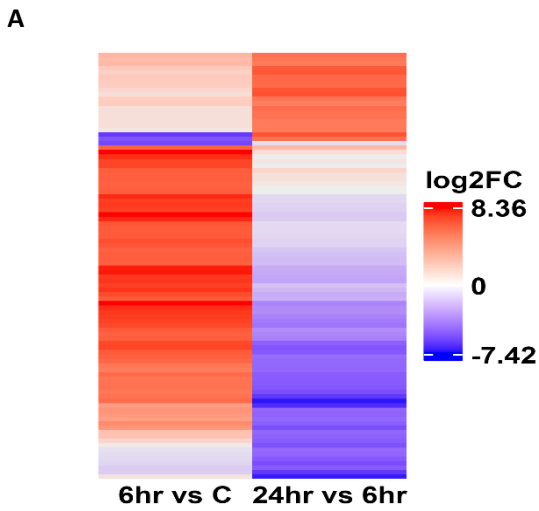


Figure 2. Heatmap displaying differentially expressed genes in stimulated and restimulated experimental groups [A]. BMDM from the 6-hour vs. control group, as well as the 24-hour vs. 6-hour group were compared to demonstrate the genes that are upregulated (red) or downregulated (blue). Volcano plots display the top upregulated and downregulated genes [B, C]. [B] depicts the top genes for the 6-hour vs. Control group, and [C] depicts the top genes for the 24-hour vs. 6-hour group.

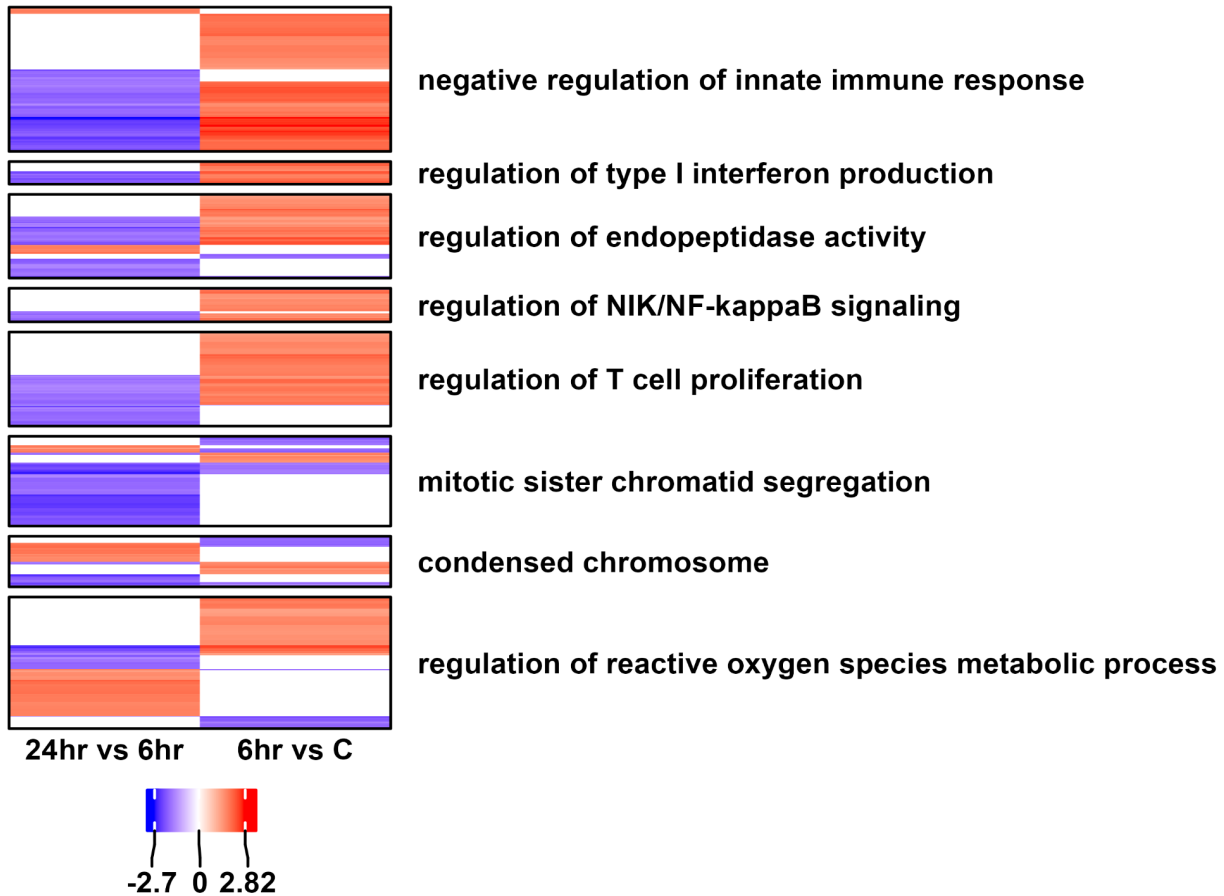


Figure 3. Heatmap displaying the PAVER clustering analysis of pathways identified as significantly dysregulated in 24hr vs 6hr or 6hr vs control groups. Rows show normalized enrichment scores (NES) of individual pathways. Clusters are annotated with PAVER-identified most representative terms.

GOID	Pathway	24hr vs 6hr	6hr vs C
GO:0001819	positive regulation of cytokine production	-2.026108965	2.541297134
GO:0032731	positive regulation of interleukin-1 beta production	-2.166431755	2.352367759
GO:0032651	regulation of interleukin-1 beta production	-2.128690795	2.291247819
GO:0032732	positive regulation of interleukin-1 production	-2.158011499	2.261213768
GO:0032652	regulation of interleukin-1 production	-2.197959624	2.200232107
GO:0032680	regulation of tumor necrosis factor production	-1.954602603	2.264451938
GO:1903555	regulation of tumor necrosis factor superfamily cytokine production	-1.949986019	2.2634614
GO:0032760	positive regulation of tumor necrosis factor production	-1.904606128	2.292463616
GO:0032479	regulation of type I interferon production	-2.084652961	2.101028638
GO:1903557	positive regulation of tumor necrosis factor superfamily cytokine production	-1.887622168	2.272065693

Table 1. Table showing select pathways in the regulation of type-I interferon production cluster. This table shows the ten highest changes in pathway dysregulation between the 6hr vs C and the 24hr vs 6hr. The table includes: the GO ID, pathway, normalized enrichment score (NES) at 24hr vs 6hr and at 6hr vs control.

Perturbagen	Similarity	MOA	Gene Targets	Cell	Tissue	Concentration	Time	FDA Phase
PHA-793887	0.65	CDK inhibitor	CDK1 CDK10 CDK11B CDK12 CDK13 CDK14 CDK15 CDK16 CDK17 CDK18 CDK19 CDK2	BT20	breast	3.33uM	24h	1
Palbociclib	0.632	CDK inhibitor	CCND1 CDK4 CDK6	MDAMB231		10uM	24h	4
Cladribine	0.631	Adenosine deaminase inhibitor	ADA	VCAP	prostate	10uM	6h	4
Pevonedistat	0.626	Nedd activating enzyme inhibitor	NAE1 UBA3	HELA	large intestine	1.11uM	24h	2
O-Demethylated Adapalene	0.609	Retinoid receptor agonist	RARG	VCAP	prostate	10uM	6h	
Gemcitabine	0.598	Ribonucleotide reductase inhibitor	POLA1 POLD1 POLE RRM1 RRM2 RRM2B	VCAP	prostate	0.1uM	6h	4
Wortmannin	0.598	PI3K inhibitor	PIK3CA PIK3CG PLK1	VCAP	prostate	10uM	24h	
Fludarabine	0.595	DNA synthesis inhibitor	RRM1	VCAP	prostate	10uM	6h	
CGK733	0.585	ATM kinase inhibitor ATR kinase inhibitor	ATM ATR	HUVEC	umbilical vein	10uM	24h	
Niclosamide	0.583	DNA replication inhibitor STAT inhibitor	STAT3	HT29	large intestine	10uM	24h	4

Table 2. Top LINCS Concordant Signatures for 24 hr vs 6hr groups. Top concordant chemical perturbagens from the LINCS database, potentially enhancing macrophage tolerance effects induced by *Borrelia burgdorferi*.

Perturbagen	Similarity	MOA	Gene Targets	Cell	Tissue	Concentration	Time	FDA Phase
SCHEMBL1564574	-0.576	CHK inhibitor	CHEK1 CHEK2	MCF7	breast	1uM	6h	
VU0365118-1	-0.505			VCAP	prostate	10uM	24h	
Parbendazole	-0.501	Tubulin inhibitor	TUBB	VCAP	prostate	0.5uM	24h	
MLS000925170	-0.499			VCAP	prostate	10uM	24h	
CHEMBL3188661	-0.495	DDR1 inhibitor	DDR1	ASC.C		1.11uM	24h	
Docetaxel Intermediate	-0.492	Tubulin inhibitor	TUBB	VCAP	prostate	10uM	24h	
Podofilox	-0.49	Microtubule inhibitor Tubulin inhibitor		VCAP	prostate	10uM	24h	4
ZINC01792951	-0.49			VCAP	prostate	10uM	24h	
Tivantinib	-0.483	Tyrosine kinase inhibitor	MET	NPC	neural progenitor cells	1.11uM	24h	3
Triazolothiadiazine, 9	-0.483	Phosphodiesterase inhibitor		VCAP	prostate	10uM	24h	

Table 3. Top LINCS Discordant Signatures for 24 hr vs 6hr groups. Top discordant chemical perturbagens identified in the LINCS database, potentially reversing macrophage tolerance effects induced by *Borrelia burgdorferi*.